Cell Host & Microbe
Resource

Chlamydia trachomatis-Induced Alterations in the Host Cell Proteome Are Required for Intracellular Growth

Andrew J. Olive,[1] Madeleine G. Haff,[1] Michael J. Emanuele,[2,3,4] Laura M. Sack,[2,3,4] Jeffrey R. Barker,[5] Stephen J. Elledge,[2,3,4] and Michael N. Starnbach[1,*]
[1]Department of Microbiology and Immunobiology, Harvard Medical School, Boston, MA 02115, USA
[2]Department of Genetics, Harvard Medical School, Boston, MA 02115, USA
[3]Division of Genetics, Brigham and Women's Hospital, Boston, MA 02215, USA
[4]Howard Hughes Medical Institute
[5]Department of Microbiology and Molecular Genetics, Duke University Medical School, Durham, NC 22710, USA
*Correspondence: starnbach@hms.harvard.edu
http://dx.doi.org/10.1016/j.chom.2013.12.009

SUMMARY

Intracellular pathogens directly alter host cells in order to replicate and survive. While infection-induced changes in host transcription can be readily assessed, posttranscriptional alterations are more difficult to catalog. We applied the global protein stability (GPS) platform, which assesses protein stability based on relative changes in an adjoining fluorescent tag, to identify changes in the host proteome following infection with the obligate intracellular bacteria *Chlamydia trachomatis*. Our results indicate that *C. trachomatis* profoundly remodels the host proteome independently of changes in transcription. Additionally, *C. trachomatis* replication depends on a subset of altered proteins, such as Pin1 and Men1, that regulate the host transcription factor AP-1 controlling host inflammation, stress, and cell survival. Furthermore, AP-1-dependent transcription is activated during infection and required for efficient *Chlamydia* growth. In summary, this experimental approach revealed that *C. trachomatis* broadly alters host proteins and can be applied to examine host-pathogen interactions and develop host-based therapeutics.

INTRODUCTION

Pathogens manipulate host cells for survival, intracellular replication, and transmission (Ham et al., 2011; Rohmer et al., 2011). Many intracellular pathogens translocate virulence factors into the host cytosol (Bingle et al., 2008; Cornelis, 2010), which is important for survival and replication (Barry et al., 2011; Cossart and Roy, 2010). Redundancy in the effector repertoire and targeted host pathways is a complicating factor in our understanding of how bacterial effectors function (Galán, 2009; O'Connor et al., 2011). Although transcriptional profiling has been an important tool for studying host-pathogen interactions (Burrack and Higgins, 2007), the host response to infection and the function of effectors cannot be determined by microarray analysis alone because many bacterial effectors act posttranscriptionally to modify or alter the stability of host proteins directly (Ensminger and Isberg, 2010; Misaghi et al., 2006; Mukherjee et al., 2006).

The obligate intracellular bacterium *Chlamydia trachomatis* is a leading cause of bacterial sexually transmitted disease and preventable blindness worldwide (Holmes, 2008). The elementary body (EB) is the infectious form of *C. trachomatis* that develops into the replicative form, called the reticulate body (RB), upon uptake into host cells (Moulder, 1991). Replication occurs within a specialized vacuole known as the inclusion. A type III secretion system (TTSS) is used by *C. trachomatis* to deliver bacterial effectors into the host cytosol during intracellular infection (Peters et al., 2007). Proteins delivered into the cytosol by *C. trachomatis* include two deubiquitinating enzymes and several proteases. This suggests that *C. trachomatis* directly manipulates host protein turnover during infection; however, the targets and activities of most secreted effectors remain largely unknown (Chellas-Géry et al., 2007; Misaghi et al., 2006; Zhong, 2011).

Our understanding of the manipulation of host proteins by *C. trachomatis* would benefit from an analysis of host cell protein turnover; however, the methods available to study global changes to host proteins following infection are limited. Thus, we adapted the global protein stability (GPS) platform to screen the human ORFeome following infection with *C. trachomatis* (Emanuele et al., 2011; Yen et al., 2008). Hundreds of host proteins that are altered in stability during infection were identified, which led to the elucidation of host pathways that are manipulated during infection. Thus, GPS screening is a powerful approach that can be applied to the study of bacterial effectors and for the identification of host pathways manipulated posttranscriptionally during pathogen infection.

RESULTS

The Global Protein Stability Platform Identifies Hundreds of Host Proteins that Are Altered Following Infection with *C. trachomatis*

To search for host proteins whose stability is altered following infection with *C. trachomatis*, we adapted the GPS screening platform. GPS is a system originally designed as a fluorescent

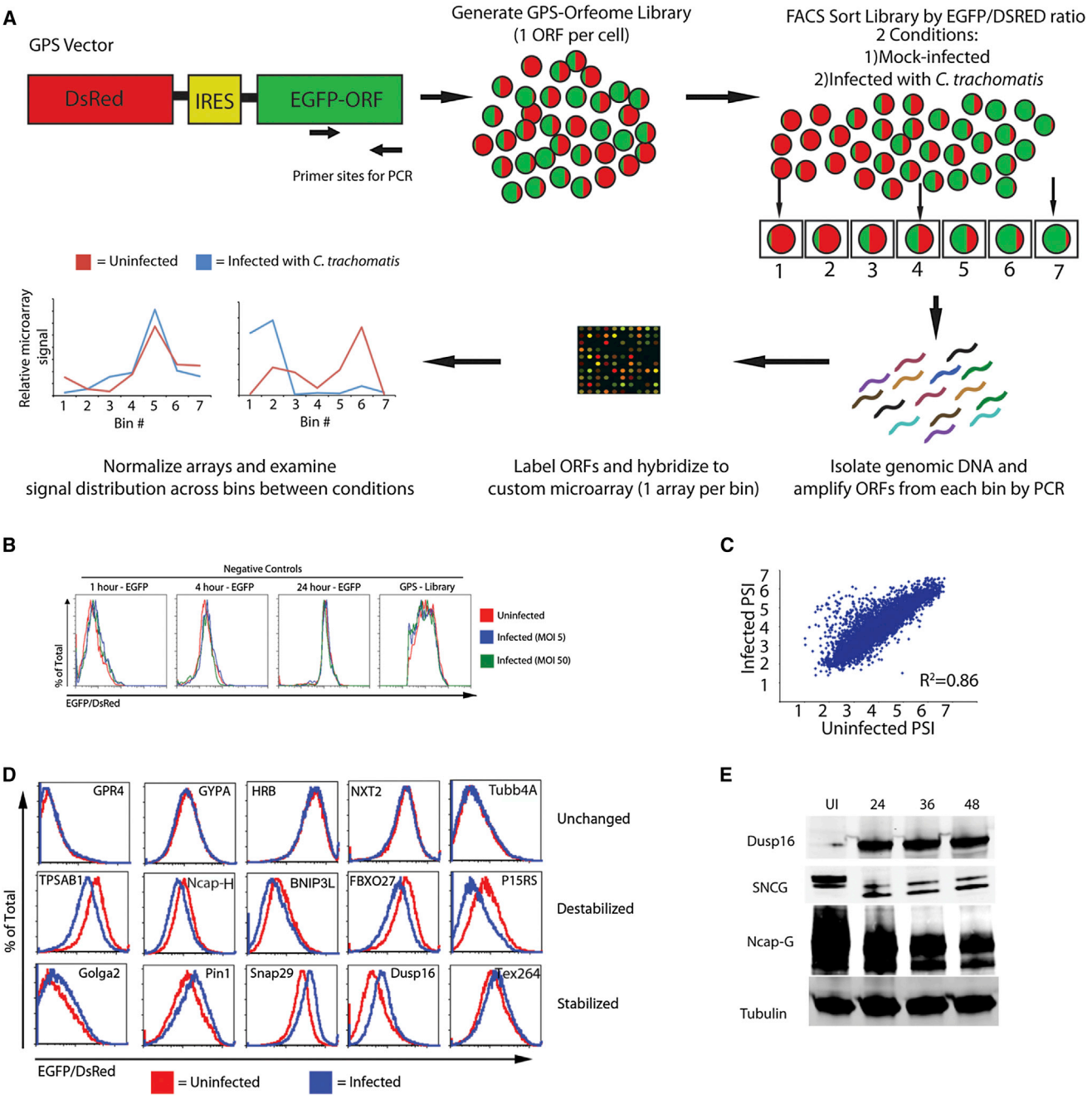

Figure 1. GPS Profiling Identifies Host Proteins Altered during *C. trachomatis* Infection

(A) Schematic representation of the GPS screen (adapted from Emanuele et al., 2011).

(B) Histograms show the EGFP/DsRed ratio for cells expressing GFP for varying half-lives and the entire GPS library. The cell lines were mock infected (red line) or infected with *C. trachomatis* at an moi of 5 (blue line) or 50 (green line) for 24 hr and analyzed by flow cytometry.

(C) Scatter plot for the PSI for each probe in the screen under the two conditions (mock infected versus infected).

(D) A subset of candidates that were tested by expressing the host gene in HEK293T cells. Cells were mock infected (red line) or infected with *C. trachomatis* (blue line) for 24 hr and evaluated using flow cytometry. Shown is a representative plot from three independent experiments.

(E) HEK293T cells were mock infected or infected with *C. trachomatis* for the indicated amount of time. Cells were analyzed by immunoblot for the expression of the experimental proteins (Dusp16, SNCG, and NCAP-G) as well as β-tubulin (loading control). Blots are representative of at least three independent experiments.

See also Figure S1 and Tables S1, S2, and S4.

protein-based method to identify the substrates of mammalian ubiquitin ligases (Emanuele et al., 2011; Yen et al., 2008). The GPS library was assembled from an arrayed set (ORFeome v3.1) of 12,000 human open reading frames (ORFs), each engineered into a retroviral reporter construct whose general structure is shown in Figure 1A (Emanuele et al., 2011). The

reporter expression cassette contains a single pCMV promoter and an internal ribosome entry site (IRES), permitting the translation of two fluorescent proteins from one mRNA transcript. The first fluorescent protein is the internal control DsRed, and the second is an enhanced GFP (EGFP) expressed as a fusion to one of 12,000 host cell proteins. When integrated into the genome of cells, DsRed and EGFP-X are produced at a constant ratio (independent of transcriptional regulation) because they are translated from the same mRNA and lack regulatory 5′ and 3′ UTRs. However, once translated, the amount of DsRed remains constant, but the level of EGFP changes based on the stability of the protein fused to its C terminus. When measured by flow cytometry, this baseline EGFP:DsRed ratio reflects relative protein stability: the lower the ratio, the less stable the protein fused to EGFP.

Prior to running the GPS screen, we confirmed that infection with *C. trachomatis* does not alter the inherent stability of EGFP or DsRed. First, we infected cells containing the GPS cassette with EGFP of varying half-lives at a multiplicity of infection (moi) of 5 and 50 for 24 hr and then analyzed the samples by flow cytometry (Figure 1B). Overlays of the EGFP:DsRed ratio show no noticeable shifts under either infection condition, indicating that infection does not alter the fluorescent reporter proteins alone.

We next executed a full-scale GPS screen to identify host proteins that are altered in stability during infection with *C. trachomatis*. We first sorted the uninfected human embryonic kidney 293T (HEK293T) cells by high-throughput fluorescence-activated cell sorting (FACS) into seven bins, based on their individual EGFP:DsRed ratio, with increasing EGFP:DsRed ratios corresponding to bins 1–7 (low to high). The ORFs in each bin were then amplified from genomic DNA using PCR, fluorescently labeled, and hybridized to custom-designed microarrays (one microarray per bin). The intensities for each individual probe from all seven arrays were measured and graphed across all seven bins. The presence of a cell bearing a particular ORF in bins of higher numbers indicates that the protein is stable in the cells; the presence of a cell bearing a particular ORF in bins of lower numbers indicates that the protein is unstable in the cells. Using these distributions, we calculated a protein stability index (PSI) for each ORF. In a parallel experiment, we infected the HEK293T cells with *C. trachomatis* EBs at an moi of 3 for 24 hr. Using the PSI value for each protein in the library under uninfected and infected conditions, we calculated a ΔPSI resulting from infection (Yen et al., 2008). We used a priority rank system to identify high-confidence hits using a combination of ΔPSI, probe intensity, agreement among probes for a single ORF, and visual inspection of ΔPSI graphs (described in the Supplemental Experimental Procedures available online). We first compared the agreement of each probe for a given ORF between uninfected and infected conditions, which showed a linear relationship and an R^2 value > 0.85 (Figure 1C). When comparing probe distributions across the microarrays, the majority of ORFs examined were indistinguishable, increasing our confidence in shifts seen following infection (Figure S1A). We next ordered every ORF by the ΔPSI, graphed them from most stabilized (negative ΔPSI) to most destabilized (positive ΔPSI) (Figure 1C), and identified over 600 proteins (out of 8,000 that passed initial filtering from the microarrays) that are altered in stability (absolute value of ΔPSI > 0.25) following infection with *C. trachomatis* (Table S1 and described in detail in the Supplemental Experimental Procedures). This included far more proteins than we anticipated based on previously reported transcription data and suggested that *C. trachomatis* profoundly remodels the host proteome upon infection (Xia et al., 2003).

In order to both estimate robustness of the GPS screen and validate the proteins identified, we individually cloned a random subset of 175 (out of 600) unique ORFs into the GPS vector and transduced HEK293T cells. Cell lines individually expressing a single EGFP-ORF fusion were then mock infected or infected with *C. trachomatis* for 24 hr and analyzed by flow cytometry to examine changes in the EGFP:DsRed ratio. In these experiments, 109 cell lines (62%) had altered ratios following infection with *C. trachomatis* in at least two out of three replicates (Figure 1D, Table S1). To ensure that these changes accurately reflected changes at the protein level, 20 random ORFs were cloned into a retroviral FLAG-tagged vector and used to create stable cells expressing tagged versions of proteins. We chose a short epitope tag instead of EGFP to limit concern about the tag interfering with function of the protein. We then mock infected or infected these cell lines and probed for tagged proteins in uninfected and infected lysates. A total of 14 of 20 (70%) showed quantifiable changes by immunoblot, indicating the reproducibility of our results (Figure S1B). Since GPS is a screening platform that expresses each ORF independently of normal transcriptional regulation, we wanted to confirm that a subset of protein changes was occurring at endogenous levels of expression following infection with *C. trachomatis*. Using immunoblots, we examined the endogenous levels of nine proteins and found that seven were altered following infection (Figures 1E and S1C). We also confirmed several of these protein changes following infection of HeLa cells (data not shown).

Interestingly, we found that while the GFP fusions accurately informed us when a specific protein was altered, they did not always predict whether a protein was stabilized or destabilized. For example, we identified the host protein SNCG as stabilized following infection with *C. trachomatis* using the GPS reporter, yet immunoblot analysis showed that this protein is actually cleaved following infection (Figures 1D and 1E). These data suggest that cleavage of host proteins in the GPS platform can remove specific degrons, leading to the stabilization of the EGFP reporter even though cleavage has occurred.

To help integrate our GPS hit data into the overall biology of the host cell, we conducted bioinformatics analysis using the database for annotation, visualization, and integrated discovery (DAVID) clustering analysis (details in Supplemental Experimental Procedures) (Huang et al., 2009). Many proteins in enriched clusters recapitulated previous studies of *Chlamydia* infection (Table S2). These included chromatin remodeling proteins, the Golgi apparatus, cell cycle control proteins, and host cytoskeleton networks, indicating that our GPS data can identify pathways important for *Chlamydia* growth (Table S2) (Balsara et al., 2006; Chumduri et al., 2013; Heuer et al., 2009; Hybiske and Stephens, 2007; Rejman Lipinski et al., 2009). Top clusters that include protein families not previously associated with *Chlamydia* infection contained transcription factors and host-signaling cascades such as c-Jun N-terminal kinase (JNK) (Table S2). Additionally, a number of altered proteins

were enriched in the nuclear membrane or mitochondria, suggesting that *Chlamydia* infection directly alters the makeup of these intracellular organelles (Table S2).

We next used the data from the GPS screen and our bioinformatics analysis to execute a small-scale proof-of-principle study to test the whether the subtler interactions we identified could reveal broader infection-induced alterations to host pathways. To do this, we mined the GPS data set for proteins that had robust shifts in EGFP:DsRed and were members of a larger family of proteins that were otherwise not identified in the screen. Two protein families we explored were the dual-specificity phosphatases (Dusps) and nuclear pore proteins (Nups) that both had family members shift (Dusp15/16 and Nup50/160) (Table S1), but did not have broad coverage of the entire protein family. To test whether *Chlamydia* infection more broadly alters this protein family, we cloned a larger panel of Dusps (12 members) and Nups (8 members) into the GPS vector and created stable reporter cell lines for each member. We then infected these cells with *Chlamydia* and examined the shift of EGFP:DsRed 24 hr later by flow cytometry. We found that infection with *Chlamydia* broadly influenced the stability of 11 out of 12 Dusps and 6 out of 8 Nups, suggesting that this family of proteins may be broadly altered during infection (Figure S2). Hence, the GPS platform can drive additional studies that reveal mechanisms in play during *Chlamydia* interaction with the host.

Knockdown of a Subset of Altered Host Proteins Inhibits the Growth of *C. trachomatis*

To assess the functional consequences of *C. trachomatis*-induced altered protein stability, we employed RNAi-mediated depletion of host proteins that were stabilized during *C. trachomatis* infection. If stabilization of these proteins is important for the intracellular developmental process, then we would predict that depletion of these proteins would have a deleterious effect on bacterial growth or replication. We optimized this screen using siRNAs to PTEN, as it has been previously shown that PTEN depletion leads to decreased bacterial growth (Figure S2) (Gurumurthy et al., 2010). Cells were transfected with pools of 4 siRNAs for 72 hr, infected with *C. trachomatis*, and subsequently evaluated for bacterial growth by measuring the production of infectious progeny (inclusion forming units, IFUs). We conducted a siRNA screen of 200 genes in triplicate, including 147 host genes stabilized during infection and 50 genes whose stability was not affected by infection. Of the 147 genes whose stability was altered by *Chlamydia*, depletion of 26 of them resulted in a decrease of at least 2-fold in *C. trachomatis* growth as assessed by IFU analysis. In contrast, depletion of only 2 out of 50 of the control proteins affected *C. trachomatis* growth, suggesting enrichment among stabilized proteins of host proteins essential for bacterial growth (Table S3). To further validate these findings, we conducted an RNAi screen with 4 individual duplexes per gene, and we identified 13 host genes whose knockdown inhibited *C. trachomatis* growth with at least two independent duplexes (Table S3). These data illustrate that a subset of host proteins that were identified as stabilized following infection are required for normal *Chlamydia* growth and suggest that these are host proteins or pathways that could be targets for host-based therapeutics.

As an alternative knockdown method, we selected three genes (Pin1, Men1, and MAGEA11) that were stabilized in the GPS screen and created stable knockdown cell lines using two independent lentivirus-delivered shRNAs for each gene of interest or for control genes. Pin1 and Men1 are involved in regulating the magnitude host signaling networks, including AP-1, while MAGEA11 regulates hypoxia-inducible factor 1α (HIF1α) activity (Aprelikova et al., 2009; Ikeo et al., 2004; Lee et al., 2009; Monje et al., 2005). Both cellular functions have been implicated as important during *C. trachomatis* infection, and we wanted to confirm their role. Positive transductants were selected with puromycin, and knockdown was confirmed using immunoblot (Figure S2E). We then examined the ability of *C. trachomatis* to replicate and produce infectious progeny in each knockdown cell line using two distinct assays: qPCR to quantify the number of *Chlamydia* genomes present and titration of infected lysates to measure IFU production. This allowed us to simultaneously query the entire *Chlamydia* life cycle, including redifferentiation into EBs. When we examined the levels of *C. trachomatis* by qPCR, we found modest, but reproducible, 1.5- to 2-fold defects in replication in each knockdown (Figure 2B). However, these deficiencies were amplified when we examined the production of infectious progeny, with some knockdowns causing a reduction of almost 10-fold in IFU (Figures 2C and 2D). We also examined the development of inclusions in knockdown cells by fluorescence microscopy. At 30 hr after infection, there was no significant difference in the morphology of inclusions between control and experimental knockdown cells. When we quantified inclusion size, there was trend toward smaller inclusions, yet not of statistical significance. This suggests that the pathways interacting with these host proteins may be required for late bacterial replication and/or the redifferentiation of RBs to EBs (Figure S2). Together, these data confirm that a subset of proteins that are stabilized during infection with *C. trachomatis* are also required for intracellular growth of the pathogen.

AP-1-Dependent Transcription Is Activated following Infection with *C. trachomatis*

The bioinformatics analysis of the GPS screen showed a strong enrichment in kinase signaling cascades and transcription factors. When we individually examined the role of the 13 genes identified in the loss-of-function screen using natural language processing, we also found several genes, including Pin1 and Men1, that directly influence the activation and amplitude of the host transcription factor AP-1 (Chen et al., 2009; Chittenden et al., 2008; Ikeo et al., 2004; Park et al., 2012) (Figure S3). AP-1 is a heterodimeric transcription factor usually made up of a Jun and Fos protein that, together, regulate the expression of a large range of host genes related to inflammation, stress, and cell survival (Schonthaler et al., 2011). The AP-1 complex is activated following infection with a wide range of bacterial pathogens, but its role in *C. trachomatis* intracellular growth has not been described. Both Pin1 and Men1 have been shown to augment c-Jun signaling in human cells (Ikeo et al., 2004; Lee et al., 2009; Monje et al., 2005). Pin1, which is a prolyl isomerase, stabilizes phosphorylation-dependent signaling events through the isomerization of phosphorylated proteins (Lee et al., 2009; Monje et al., 2005). Men1 prevents transcription of the AP-1 component JunD but augments the signaling cascades driven

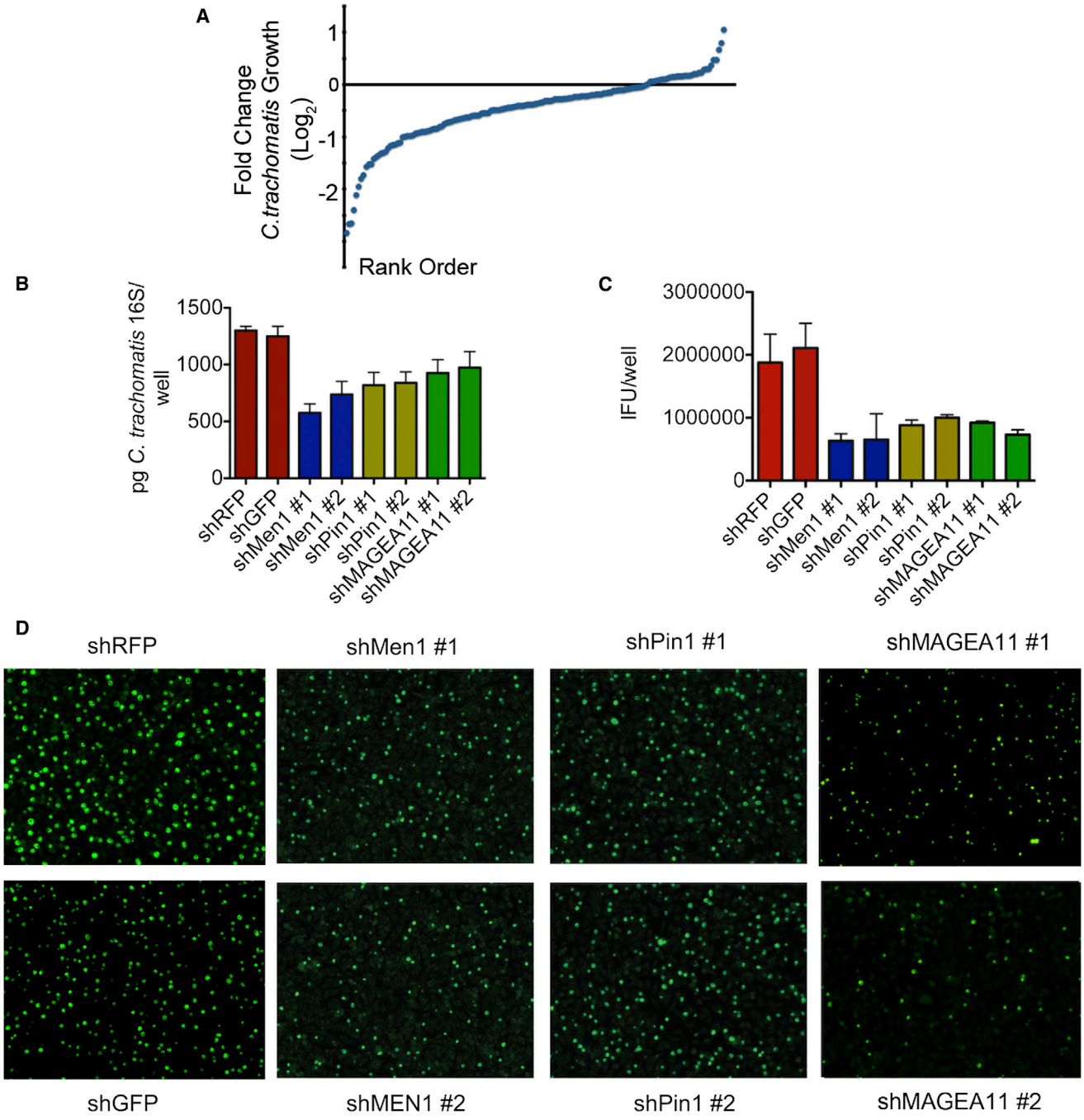

Figure 2. Loss-of-Function Screen Identifies Host Proteins that Are Necessary for *C. trachomatis* Propagation

(A) Distribution of the mean fold change in *C. trachomatis* IFU production in experimental siRNA knockdown cell lines relative to negative controls.

(B) A subset of stable shRNA knockdown cell lines was infected with *C. trachomatis* for 48 hr. Levels of *C. trachomatis* were determined by qPCR of the 16S gene and compared to nontargeting controls. The graphs show the mean levels of *C. trachomatis* from two independent hairpins ± SD. Shown is one of four independent experiments (n = 4).

(C) A subset of stable shRNA knockdowns was infected with *C. trachomatis* for 48 hr. Levels of *C. trachomatis* were determined by IFU production and compared to nontargeting control hairpins. The graphs show the mean IFU of *C. trachomatis* produced ± SD for each individual hairpin. All experimental hairpins are $p < 0.05$ compared to control knockdown by one-way ANOVA. Shown is one of four independent experiments (n = 4).

(D) Representative immunofluorescence micrographs from IFU analysis (10× magnification) from one of three independent experiments (n = 3). See also Figure S2 and Table S3.

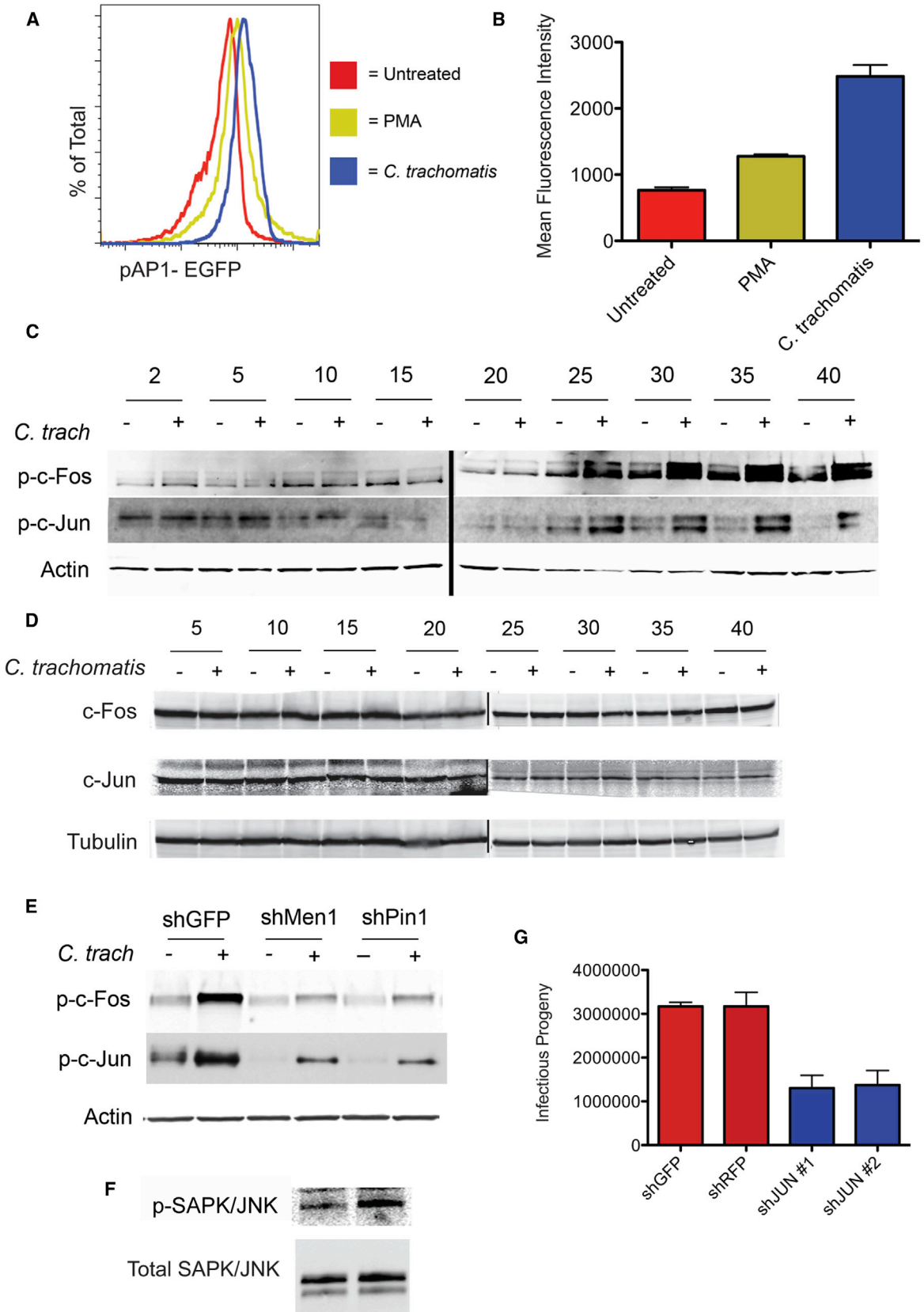

(legend on next page)

by c-Jun (Ikeo et al., 2004). Therefore, the stabilization of both Pin1 and Men1 protein during *Chlamydia* infection would enhance c-Jun/c-Fos-dependent AP-1 signaling. We first examined whether changes in AP-1-dependent transcription occurred following infection by *C. trachomatis* by using a reporter cell line that expresses EGFP in an AP-1-dependent manner. We mock treated these reporter cells, treated cells with PMA (phorbol-12-myristate-13-acetate, a known activator of AP-1-driven transcription), or infected them with *C. trachomatis*. At 36 hr after infection, we analyzed cells by flow cytometry in order to determine the levels of EGFP. Relative to untreated controls, there was distinct upregulation of EGFP in *Ct*-infected cells, which was even more pronounced than that in PMA-treated cells (Figure 3A). Quantification revealed an increase greater than 3-fold in the mean fluorescence intensity (MFI) of EGFP in *Chlamydia*-infected cells compared to control cells (Figure 3B). These data show that, following infection with *C. trachomatis*, AP-1-directed transcription is activated.

The phosphorylation of the AP-1 components c-Jun and c-Fos is required for AP-1-dependent transcription, so we next examined these phosphorylation events in cells infected with *C. trachomatis*. We mock infected or infected HeLa cells with *C. trachomatis* and examined the levels of total and phosphorylated c-Jun and c-Fos by immunoblot every 5 hr throughout infection (Figure 3C). Cells infected with *C. trachomatis* showed minimal phosphorylation of c-Fos or c-Jun for the first 20 hr of infection. However, 20–25 hr after infection, there was a significant increase in the phosphorylation of both c-Fos and c-Jun that increased in magnitude through the remainder of the time course (Figure 3C). When we examined the levels of total c-Jun and c-Fos, we found minimal changes in the basal levels of both proteins throughout infection with *C. trachomatis* (Figure 3D). These experiments validated our findings using the AP-1 reporter and showed that AP-1 is activated late in host cells infected with *C. trachomatis*.

We next confirmed the timing of AP-1 activation by examining the transcriptional activation of two known AP-1 targets using quantitative RT-PCR. HeLa cells were mock infected or infected with *C. trachomatis* for 20 or 30 hr. Cells were then lysed, and RNA was purified for expression analysis. Using premixed primer pairs, we amplified individual genes by RT-PCR in technical duplicates to analyze changes in transcription. Experimental genes were then normalized to host β-actin expression, and the fold change in infected cells was determined. In line with our immunoblot analysis, we saw no changes in mRNA levels of two AP-1 target genes, c-Fos or JunB, 20 hr after infection or at any earlier time points examined (Figure S3 and data not shown). However, 30 hr after infection, we saw a strong induction of the expression of both c-Fos and JunB mRNA. These data support our findings that AP-1-dependent transcription is activated between 20 and 30 hr following *C. trachomatis* infection.

Because our loss-of-function screen identified genes that altered *C. trachomatis* growth and also influence AP-1 signaling (Figure S3), we were curious whether *Chlamydia* restriction in these knockdown cells might be due in part to alterations in the activation of AP-1. To test this, we mock infected or infected stable control knockdown cells or cells containing shRNA against Men1 or Pin1 with *C. trachomatis* for 40 hr. Cells were then lysed and probed for the activation of AP-1 components by immunoblot. Both shPin1 and shMen1 knockdown cells showed a significant decrease in the phosphorylation of c-Fos and c-Jun (Figure 3E) compared to shGFP controls. These data show a direct link between the loss-of-function data and the activation of the AP-1 signaling cascade and suggest one potential mechanism preventing efficient *Chlamydia* growth in these cells.

If AP-1-dependent transcription is required for *C. trachomatis* growth, we hypothesized that upstream signaling components, such as the mitogen-activated protein kinase (MAPK) pathways p38, ERK, and JNK, would also be activated during infection. These pathways have previously been shown to mediate c-Jun phosphorylation, and both p38 and ERK are activated throughout infection with *C. trachomatis* (Buchholz and Stephens, 2007; Chen et al., 2010). One previous study showed that inhibition of ERK and p38 leads to continued c-Jun phosphorylation (Chen et al., 2010), but we hypothesized that the JNK pathway may also play a role in this process. Two previous studies examined JNK activation early following infection with *C. trachomatis* and did not observe activation. However, these reports may have overlooked subtle activation of this cascade that occurs later during infection (Buchholz and Stephens, 2007; Chen et al., 2010). Therefore, we examined JNK activation throughout infection with *C. trachomatis*. We infected HeLa cells with *C. trachomatis* and then lysed the cells at various time points. These lysates were then used to perform a sandwich

Figure 3. *C. trachomatis* Infection Leads to the Activation of the AP-1 Complex

(A) pAP-1 EGFP reporter cells were mock infected, infected with *C. trachomatis*, or treated with PMA. Then, 30 hr later, EGFP expression was determined by flow cytometry. A representative plot overlaying the three conditions is shown from three experiments (n = 3).

(B) Quantification of the mean fluorescence intensity for each condition from (A) ± SD (n = 3). Both PMA and infection are $p < 0.05$ compared to mock by two-tailed Student's t test. Shown is a representative experiment from three completed experiments.

(C) Immunoblot analysis of phosphorylated c-Fos (top) and c-Jun (bottom) in mock-infected HeLa cells or HeLa cells infected with *C. trachomatis* every 5 hr for 40 hr. Loading was normalized to actin. Shown is a representative blot from one of three independent experiments.

(D) Total c-Jun and c-Fos remain unchanged during infection with *Chlamydia*. HeLa cells were infected with *Chlamydia* or mock infected. At the indicated time points, cells were lysed and analyzed for total levels of c-Fos and c-Jun. All lysates were normalized using tubulin. Shown is a representative blot from three independent experiments.

(E) Indicated shRNA knockdown cells were infected or mock infected with *Chlamydia* for 40 hr. Cells were lysed, and the levels of phosphorylated c-Fos and c-Jun were determined by immunoblot. Loading was normalized to host actin. Shown is a representative blot from one of three independent experiments.

(F) Immunoblot analysis of HeLa cells infected mock infected or infected with *C. trachomatis* for 30 hr to determine the levels of total SAPK/JNK (bottom) and phosphorylated SAPK/JNK (top). Shown is a representative blot from four independent experiments.

(G) shJUN knockdowns were infected with *C. trachomatis* for 48 hr. Levels of *C. trachomatis* were determined by IFU production and compared to nontargeting control hairpins. The graphs show the mean IFU of *C. trachomatis* produced ± SD for each individual hairpin (n = 6). Shown is one representative experiment from two completed experiments. All experimental hairpins have $p < 0.05$ compared to control knockdown by one-way ANOVA. See also Figure S3.

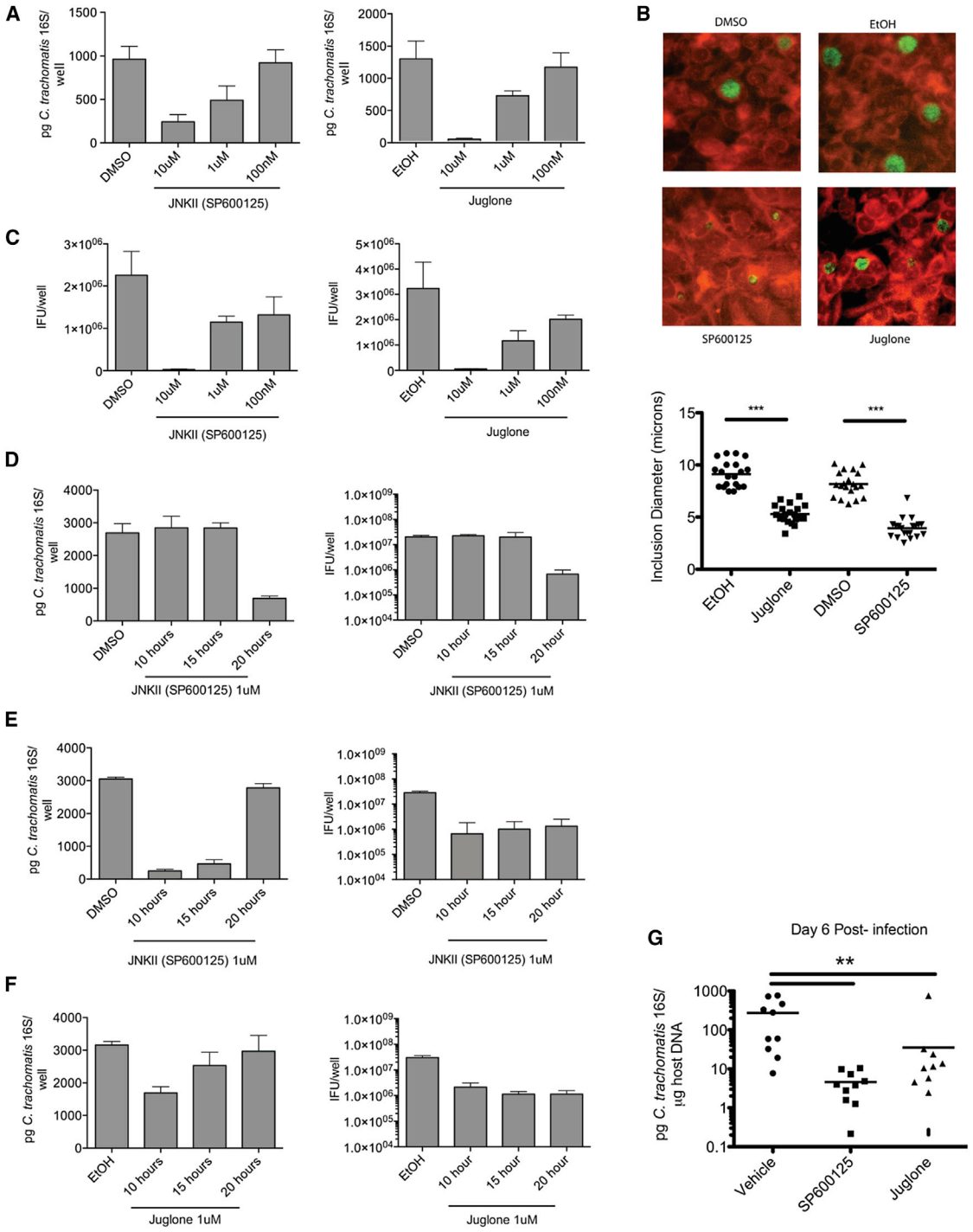

Figure 4. Inhibition of AP-1 Signaling Prevents *C. trachomatis* Growth and the Production of Elementary Bodies

(A) HeLa cells were infected with *C. trachomatis* and then treated with the indicated concentration of JNK inhibitor (SP600125), Pin1 inhibitor (juglone), or vehicle alone (DMSO or EtOH). The number of *Chlamydia* genomes was quantified using qPCR at 48 hr after infection. Shown is a representative experiment of four completed experiments (n = 4). All experimental inhibitor treatments, except 100 nM, are $p < 0.05$ compared to vehicle control by one-way ANOVA.

(B) Infected HeLa cells were treated with vehicle alone or the indicated inhibitors and fixed 30 hr after infection. Cells were stained for *C. trachomatis* major outer membrane protein (MOMP). Top: representative images of *C. trachomatis* inclusions treated with DMSO, EtOH, SP600125, or juglone (10 μM each at 20× magnification) from one of two independent experiments. Bottom: quantification of average inclusion diameter following inhibitor treatment. $p < 0.001$ by Student's t test (n = 20).

(C) Production of IFU from cells infected with *C. trachomatis* then treated with the indicated inhibitors for 48 hr (n = 4). All experimental inhibitor treatments are $p < 0.05$ compared to vehicle control by one-way ANOVA. Shown is a representative experiment of four independent experiments.

(legend continued on next page)

ELISA to detect total levels of SAPK/JNK as well as phosphorylated levels of SAPK/JNK. We found that following infection with *Chlamydia* there was a negligible change in the levels of total SAPK/JNK (Figure S3). However, there was a general accumulation in the levels of phosphorylated SAPK/JNK that increased as infection progressed, similar to what was observed with c-Fos and c-Jun (Figure S3). We confirmed these findings by immunoblot and determined that infection with *C. trachomatis* leads to the phosphorylation of SAPK/JNK, compared to mock-treated cells (Figure 3F). Taken together, these data show that infection with *C. trachomatis* induces AP-1-dependent transcription late in the developmental cycle and may be influenced by the JNK signaling cascade.

Since AP-1 complex regulators and robust AP-1 activation were found to be required for normal *Chlamydia* growth (Figure 2), we next directly tested the necessity of AP-1 components for *Chlamydia* replication. We created shRNA knockdowns of c-Jun using two independent hairpins (Figure S3) and compared the production of infective *C. trachomatis* progeny in these cells compared to control shRNA knockdowns (Figure 3G). Consistent with the knockdowns of AP-1-regulating components (Figures 2D and 2E), depletion of c-Jun significantly reduced the production of IFU. These data confirm that AP-1 is activated late during infection and required for *C. trachomatis* to efficiently complete its developmental cycle.

AP-1 Activation Is Required for *C. trachomatis* Growth In Vitro and In Vivo

One goal of the GPS screen was to identify host proteins or pathways that are possible targets of small molecules in order to develop host-based therapeutics that inhibit bacterial growth. As shown above, the AP-1 complex is activated during infection with *C. trachomatis,* and through loss-of-functions screens we identified that AP-1 activation is required for growth. To test whether pharmacological inhibitors of this pathway inhibit the growth and replication of *C. trachomatis*, we used two distinct inhibitors to prevent AP-1-dependent transcription: SP600125 and juglone (Figure S4). SP600125 is a JNK inhibitor that blocks upstream activation of the AP-1 complex, while juglone is a specific inhibitor of Pin1 and prevents prolonged amplification of AP-1-dependent transcription (Lee et al., 2009). We first tested the specificity of these inhibitors in infected cells by using phosphoarray analysis. Infected cells treated with 1 μM SP600125 or juglone did not alter the activation of a wide range of host pathways during infection. We also examined the phosphorylation of c-Jun by immunoblot 40 hr after infection for all conditions. In the presence of either SP600125 or juglone, there was a significant decrease in the phosphorylation of c-Jun compared to the vehicle control, indicating that the inhibitors directly alter AP-1 signaling. While these findings do not eliminate the possibility of potential off-target effects not included in our analysis, they suggest that the inhibition of c-Jun phosphorylation is partially dependent on JNK signaling.

We next infected HeLa cells with *C. trachomatis* for 1 hr and then added media containing various concentrations of SP600125, juglone, or the vehicle in which they were prepared (DMSO or EtOH alone). We examined bacterial replication using qPCR 48 hr following infection. The presence of either SP600125 or juglone at concentrations of 1 μM or higher significantly decreased the levels of *C. trachomatis* by qPCR at 48 hr after infection (Figure 4A), yet low concentrations of either inhibitor (100 nM) did not alter *C. trachomatis* growth compared to control treatments. When we examined inclusions using immunofluorescence microscopy, we noted a significant decrease in the size of inclusions in the presence of inhibitors (Figure 4B). These data suggest that inhibiting AP-1 activation can directly alter *C. trachomatis* growth.

We next examined IFU production following treatment with these compounds and found that either inhibitor significantly decreased the production of infectious progeny at all concentrations tested (Figure 4C). This was surprising based on our data showing no growth defect as measured by qPCR when using 100 nM concentrations of either inhibitor, yet these data were consistent with those obtained using shRNA knockdowns, where the defects in replication were also more pronounced when measured as IFU (Figures 2C and 2D). We further inhibited infectious progeny production by combining both inhibitors, even at low concentrations (Figure S4). Since our *Chlamydia* infection time course revealed late activation of AP-1, we conducted a washout experiment to remove the inhibitor at certain time points after infection. Because juglone is a nonreversible inhibitor, we chose to run these experiments only with the reversible JNK inhibitor. Cells were infected with *C. trachomatis* in the presence of 1 μM SP600125 or DMSO. At 10, 15, or 20 hr after infection, the media was removed, cells were washed, and fresh media lacking the inhibitor was added. After allowing the infection to continue to 48 hr, the cells were lysed, and the levels and infectivity of *C. trachomatis* were determined by qPCR and IFU titration (Figure 4D). When we removed the inhibitor as late as 15 hr after infection, we found no effect on *C. trachomatis* growth or infectivity. However, if we removed the inhibitor 20 hr following infection, we saw a profound defect in *Chlamydia*

(D) HeLa cells were infected with *C. trachomatis* and then treated with SP600125. At the indicated times after infection, the inhibitor was removed and replaced with fresh media. *C. trachomatis* levels were determined by qPCR (left) and IFU analysis (right) 48 hr after infection (n = 4). Only washout at 20 hr following infection had $p < 0.05$ compared to vehicle control by one-way ANOVA. Shown is a representative experiment of four independent experiments.
(E) HeLa cells were infected with *C. trachomatis*, and treated with SP600125at the indicated time points. At 48 hr after infection, cells were lysed and the levels of *C. trachomatis* were determined by qPCR (left) and IFU analysis (right) (n = 4). All experimental inhibitor treatments in the IFU experiment are $p < 0.05$ compared to vehicle control by one-way ANOVA. Shown is a representative experiment of four independent experiments.
(F) HeLa cells were infected with *C. trachomatis*, and then at the indicated time points the cells were treated with juglone. At 48 hr after infection, cells were lysed and the levels of *C. trachomatis* were determined by qPCR (left) and IFU production (right).
In all experiments, the graphs represent the mean level of *C. trachomatis* ± SD (n = 4). All experimental inhibitor treatments in the IFU experiment are $p < 0.05$ compared to vehicle control by one-way ANOVA. Shown is a representative experiment of four independent experiments.
(G) Mice were infected transcervically with 10^6 IFU of *C. trachomatis*. At 24, 48, and 72 hr after infection, mice were treated with the indicated inhibitors or vehicle alone. At 6 days after infection, the levels of *C. trachomatis* were determined using qPCR. Graphs show bacterial levels in individual mice and the mean distribution for each treatment group $p < 0.01$ (n = 10). Shown are the data from one of two independent experiments. See also Figure S4.

levels and IFU production. These data suggest that AP-1-dependent transcription is not required early in *C. trachomatis* infection, but it is required by 20 hr after infection.

As a complement to these experiments, we next added inhibitors at certain time points after infection. Cells were infected with *C. trachomatis*, and SP600125, juglone, or vehicle alone were added 10, 15, or 20 hr after infection. At 48 hr after infection, the cells were lysed and we determined the levels and infectivity of *C. trachomatis* by qPCR and IFU titration (Figures 4E and 4F). Similar to the washout experiment, addition of either SP600125 or juglone to infected cells at 10 or 15 hr after infection reduced *C. trachomatis* levels and IFU production. Interestingly, addition of either inhibitor 20 hr after infection had a negligible effect on the growth of *C. trachomatis* by qPCR yet caused a significant decrease in the production of IFU, similar to the defect seen following inhibitor addition at earlier time points. These data show that AP-1 signaling is required for efficient *C. trachomatis* growth in vitro.

It remained possible that the activation of AP-1 components, not AP-1-mediated transcription, was required for *Chlamydia* growth. To examine whether AP-1-mediated transcription was also required for intracellular survival, we employed a third inhibitor, Tanshinone IIA, which allows AP-1 phosphorylation but prevents DNA binding and subsequent transcriptional activity (Lee et al., 2008). Cells were infected with *C. trachomatis* for 20 hr and then treated with various concentrations of Tanshinone IIA to limit the time of inhibitor treatment. Cells were then lysed at 48 hr after infection, and bacterial levels and the production of infectious progeny were determined by qPCR and IFU analysis, respectively. We saw minimal defects in bacterial growth by qPCR but observed a significant inhibition in the production of infectious progeny in a dose-dependent manner (Figure S4). These data show that preventing AP-1-mediated transcription directly inhibits the ability of *Chlamydia* to complete the developmental cycle.

We next wanted to determine whether activation of this pathway was required for *C. trachomatis* growth in vivo. We have recently described a murine model of *C. trachomatis* infection that allows the use of human *Chlamydia* strains in mice and recapitulates many aspects of human disease in the upper genital tract (Gondek et al., 2012). Using this model, mice were infected transcervically with *C. trachomatis* and, 24, 48, and 72 hr after infection, treated with vehicle alone, SP600125, or juglone by both intraperitoneal (i.p.) injection and transcervical application. At 6 days after infection, mice were sacrificed, the upper genital tract was isolated, and the burden of *C. trachomatis* in the tissue was determined using qPCR. Treatment of mice with either SP600125 or juglone led to a 10- to 100-fold decrease in the levels of *C. trachomatis* in the upper genital mucosa compared to vehicle alone (Figure 4G). This suggests that *C. trachomatis* requires AP-1-dependent signaling in order to survive in the murine upper genital mucosa. Together, these results show that *C. trachomatis* manipulates host signaling cascades that are required for bacterial growth both in vitro and in vivo.

DISCUSSION

In this report we applied GPS, a system that probes over 12,000 proteins simultaneously to evaluate how infection with the intracellular bacterial pathogen *C. trachomatis* alters host protein stability. Some of the proteins identified in the GPS screen, including the Mcl1 protein and proteins involved in histone modifications and Golgi functions, were known to be altered during infection with *Chlamydia*, validating the screen (Chumduri et al., 2013; Heuer et al., 2009; Rajalingam et al., 2008). These findings suggest that *Chlamydia* broadly remodels the host proteome during infection, most likely through a variety of mechanisms.

This technology has the potential to uncover important host therapeutic targets. Therefore, we initially targeted the AP-1 transcription complex; both bioinformatics analysis of the GPS screen and natural language processing analysis of the loss-of-function screen indicated that the AP-1 complex is activated late during *Chlamydia* infection and required for robust intracellular growth. One of the most intriguing findings was that late blockade of AP-1 activation had much more dramatic effects on IFU production than early did AP-1 blockade. This suggests that AP-1 activity may be required for RB replication and/or redifferentiation into the EB form. Perhaps the intracellular growth of *C. trachomatis* triggers host stress responses, and *C. trachomatis* senses these host stress pathways to initiate differentiation and exit from the failing host cell.

The AP-1 complex is a critical transcription factor that regulates the expression of a large range of host genes in response to diverse stimuli (Schonthaler et al., 2011). The AP-1 complex is targeted by several bacterial pathogens to alter cellular survival or prevent inflammation and cytokine production, with some pathogens preventing activation and some inducing activation of upstream host signaling cascades (Alto and Orth, 2012). Interestingly, a recent report using *C. pneumoniae* suggested that AP-1 activation is responsible for inflammation seen in vivo (Wang et al., 2012). While the effect of AP-1 on inflammation during infection in vivo remains to be confirmed for *C. trachomatis*, these data together suggest that finely tuned AP-1 signaling is required for robust intracellular growth. While our data suggest that AP-1 activity influences *C. trachomatis* infection in vivo, we do not yet know whether this is due to restriction in the epithelial cell or alterations in the subsequent immune response.

Proteomic approaches are a robust tool by which to characterize unknown host-pathogen interactions. These techniques should be of particular interest to probe the interactions of the variety of other pathogens that deliver ubiquitin-modifying proteins to the host cell cytoplasm during infection (Collins and Brown, 2010). In addition, investigators can compare changes to the proteome that occur during infection between wild-type bacteria and strains with loss or gain of function for ubiquitin-modifying enzymes. Therefore, the experimental approaches described here provide a blueprint for cataloging host proteins and pathways that are altered in stability by intracellular pathogens. These pathways may be conserved among multiple pathogens and could drive the development of therapeutics for these difficult-to-treat infections.

EXPERIMENTAL PROCEDURES

Bacterial Strains, Tissue Culture, Reagents, and Procedures

Full description of Experimental Procedures and reagents used are available in the Supplemental Information. *C. trachomatis* serovar L2 434/Bu was

propagated as done previously. To examine *C. trachomatis* levels, both IFU and qPCR procedures were performed as done previously (Gondek et al., 2012). For IFU, infected cells were lysed, titered, stained, and quantified by fluorescence microscopy as done previously. For quantitative PCR, we measured the level of genomic DNA in samples as done previously. Automated microscopy was conducted using a Cellomics ArrayScan VTI automated microscope as done previously.

For immunoblot analysis, cells were lysed in buffer containing 8 M urea, unless otherwise indicated, and separated via SDS-PAGE. For all westerns, unless indicated, the Odyssey two-color fluorescence imaging system (LI-COR) was used. Changes in protein content were quantified using Odyssey software (LI-COR) or ImageJ. All statistics were calculated using Prism Software (GraphPad), and unless indicated, one-way ANOVA with Tukey's posttest was used, with p values under 0.05 considered significant.

GPS Screening and Scoring

GPS screens were performed essentially as described (Emanuele et al., 2011). Cells were infected with *C. trachomatis* at an moi of 3, while control cells were mock infected. At 24 hr following infection, cells were detached and prepared for cell sorting. Cells were sorted into seven bins per condition, with at least one million cells per bin. Following hybridization, microarray data were normalized and filtered based on the signal:noise ratio, and a ΔPSI value was calculated. Probe distribution across bins for treated and untreated samples was graphed using the included macro.

Bioinformatic Analysis

We used DAVID bioinformatics resources to identify enriched annotation clusters within the GPS data set, as done previously (Huang et al., 2009). We uploaded our stabilized and destabilized protein lists independently into DAVID and used the human proteome as the background list. We used cluster analysis to identify redundant enriched terms for each group through several categories, including KEGG pathway and gene ontology terms.

siRNA Screen

siRNA smart pools were picked into 96-well plates from the Dharmacon siRNA genome set at the Harvard Institute of Chemistry and Cell Biology. HeLa cells were seeded at a density of 2.5×10^3 into 96-well plates and transfected in triplicate for 72 hr, when cell viability was evaluated. Cells were then infected with 10^4 IFU of *C. trachomatis* for 48 hr, lysed, diluted 1:1,000 in fresh media, and used to infect fresh HeLa cells. Then, 24 hr later, cells were fixed with MeOH stained using DAPI and a fluorescein isothiocyanate (FITC) antibody to *C. trachomatis* major outer membrane protein (MOMP; Bio-Rad). Cells were quantified by automated microscopy as done previously. The mean number of IFU produced by nontargeting controls for each plate was calculated. A fold change in *C. trachomatis* growth was calculated against the nontargeting mean for each plate. A mean fold change was then calculated for all triplicate samples.

Inhibitor Treatment

For in vitro experiments, juglone was resuspended in EtOH; for in vivo experiments, juglone was resuspended in DMSO. SP600125 and Tanshinone IIA were dissolved in DMSO for all experiments. Vehicle controls contained the appropriate solvent for each experiment. Inhibitors were used at the indicated concentrations for each experiment.

Mice and In Vivo Inhibitor Treatment

C57BL/6 mice were purchased from The Jackson Laboratory and maintained and cared for within the Harvard Medical School Center for Animal Resources and Comparative Medicine. Mice were treated with medroxyprogesterone subcutaneously 7 days prior to infection in order to normalize the estrous cycle. Mice were infected transcervically with 10^6 IFU of *C. trachomatis*. For inhibitor treatments, mice were injected i.p. and transcervically with vehicle alone, 10 mg/kg of SP600125 per injection route (Wang et al., 2004), and 1 mg/kg of juglone per injection route (Kim et al., 2010) similar to previous studies. All experiments were approved by Institutional Animal Care and Use Committee. In all experiments, ten mice per group were used.

SUPPLEMENTAL INFORMATION

Supplemental Information includes Supplemental Experimental Procedures, four figures, and four tables and can be found with this article online at http://dx.doi.org/10.1016/j.chom.2013.12.009.

ACKNOWLEDGMENTS

We thank Jörn Coers and members of the Starnbach lab for valuable discussions. Craig Roy and Samuel Miller had helpful comments on the manuscript. This work was supported by National Institutes of Health Grants R01 AI062827 and R01 AI039558 (to M.N.S.) and R01 AG11085 (to S.J.E.) as well as a grant from Vertex Pharmaceuticals (to M.N.S.). S.J.E. is an investigator with the Howard Hughes Medical Institute.

Received: April 5, 2013
Revised: September 11, 2013
Accepted: December 11, 2013
Published: January 15, 2014

REFERENCES

Alto, N.M., and Orth, K. (2012). Subversion of cell signaling by pathogens. Cold Spring Harb. Perspect. Biol. *4*, a006114.

Aprelikova, O., Pandolfi, S., Tackett, S., Ferreira, M., Salnikow, K., Ward, Y., Risinger, J.I., Barrett, J.C., and Niederhuber, J. (2009). Melanoma antigen-11 inhibits the hypoxia-inducible factor prolyl hydroxylase 2 and activates hypoxic response. Cancer Res. *69*, 616–624.

Balsara, Z.R., Misaghi, S., Lafave, J.N., and Starnbach, M.N. (2006). Chlamydia trachomatis infection induces cleavage of the mitotic cyclin B1. Infect. Immun. *74*, 5602–5608.

Barry, A.O., Mege, J.L., and Ghigo, E. (2011). Hijacked phagosomes and leukocyte activation: an intimate relationship. J. Leukoc. Biol. *89*, 373–382.

Bingle, L.E., Bailey, C.M., and Pallen, M.J. (2008). Type VI secretion: a beginner's guide. Curr. Opin. Microbiol. *11*, 3–8.

Buchholz, K.R., and Stephens, R.S. (2007). The extracellular signal-regulated kinase/mitogen-activated protein kinase pathway induces the inflammatory factor interleukin-8 following Chlamydia trachomatis infection. Infect. Immun. *75*, 5924–5929.

Burrack, L.S., and Higgins, D.E. (2007). Genomic approaches to understanding bacterial virulence. Curr. Opin. Microbiol. *10*, 4–9.

Chellas-Géry, B., Linton, C.N., and Fields, K.A. (2007). Human GCIP interacts with CT847, a novel Chlamydia trachomatis type III secretion substrate, and is degraded in a tissue-culture infection model. Cell. Microbiol. *9*, 2417–2430.

Chen, C.B., Ng, J.K., Choo, P.H., Wu, W., and Porter, A.G. (2009). Mammalian sterile 20-like kinase 3 (MST3) mediates oxidative-stress-induced cell death by modulating JNK activation. Biosci. Rep. *29*, 405–415.

Chen, F., Cheng, W., Zhang, S., Zhong, G., and Yu, P. (2010). [Induction of IL-8 by Chlamydia trachomatis through MAPK pathway rather than NF-kappaB pathway]. Zhong Nan Da Xue Xue Bao Yi Xue Ban *35*, 307–313.

Chittenden, T.W., Howe, E.A., Culhane, A.C., Sultana, R., Taylor, J.M., Holmes, C., and Quackenbush, J. (2008). Functional classification analysis of somatically mutated genes in human breast and colorectal cancers. Genomics *91*, 508–511.

Chumduri, C., Gurumurthy, R.K., Zadora, P.K., Mi, Y., and Meyer, T.F. (2013). Chlamydia infection promotes host DNA damage and proliferation but impairs the DNA damage response. Cell Host Microbe *13*, 746–758.

Collins, C.A., and Brown, E.J. (2010). Cytosol as battleground: ubiquitin as a weapon for both host and pathogen. Trends Cell Biol. *20*, 205–213.

Cornelis, G.R. (2010). The type III secretion injectisome, a complex nanomachine for intracellular 'toxin' delivery. Biol. Chem. *391*, 745–751.

Cossart, P., and Roy, C.R. (2010). Manipulation of host membrane machinery by bacterial pathogens. Curr. Opin. Cell Biol. *22*, 547–554.

Emanuele, M.J., Elia, A.E., Xu, Q., Thoma, C.R., Izhar, L., Leng, Y., Guo, A., Chen, Y.N., Rush, J., Hsu, P.W., et al. (2011). Global identification of modular cullin-RING ligase substrates. Cell *147*, 459–474.

Ensminger, A.W., and Isberg, R.R. (2010). E3 ubiquitin ligase activity and targeting of BAT3 by multiple Legionella pneumophila translocated substrates. Infect. Immun. *78*, 3905–3919.

Galán, J.E. (2009). Common themes in the design and function of bacterial effectors. Cell Host Microbe *5*, 571–579.

Gondek, D.C., Olive, A.J., Stary, G., and Starnbach, M.N. (2012). CD4+ T cells are necessary and sufficient to confer protection against Chlamydia trachomatis infection in the murine upper genital tract. J. Immunol. *189*, 2441–2449.

Gurumurthy, R.K., Mäurer, A.P., Machuy, N., Hess, S., Pleissner, K.P., Schuchhardt, J., Rudel, T., and Meyer, T.F. (2010). A loss-of-function screen reveals Ras- and Raf-independent MEK-ERK signaling during Chlamydia trachomatis infection. Sci. Signal. *3*, ra21.

Ham, H., Sreelatha, A., and Orth, K. (2011). Manipulation of host membranes by bacterial effectors. Nat. Rev. Microbiol. *9*, 635–646.

Heuer, D., Rejman Lipinski, A., Machuy, N., Karlas, A., Wehrens, A., Siedler, F., Brinkmann, V., and Meyer, T.F. (2009). Chlamydia causes fragmentation of the Golgi compartment to ensure reproduction. Nature *457*, 731–735.

Holmes, K.K. (2008). Sexually transmitted diseases, Fourth Edition. (New York: McGraw-Hill Medical).

Huang, W., Sherman, B.T., and Lempicki, R.A. (2009). Systematic and integrative analysis of large gene lists using DAVID bioinformatics resources. Nat. Protoc. *4*, 44–57.

Hybiske, K., and Stephens, R.S. (2007). Mechanisms of Chlamydia trachomatis entry into nonphagocytic cells. Infect. Immun. *75*, 3925–3934.

Ikeo, Y., Yumita, W., Sakurai, A., and Hashizume, K. (2004). JunD-menin interaction regulates c-Jun-mediated AP-1 transactivation. Endocr. J. *51*, 333–342.

Kim, S.E., Lee, M.Y., Lim, S.C., Hien, T.T., Kim, J.W., Ahn, S.G., Yoon, J.H., Kim, S.K., Choi, H.S., and Kang, K.W. (2010). Role of Pin1 in neointima formation: down-regulation of Nrf2-dependent heme oxygenase-1 expression by Pin1. Free Radic. Biol. Med. *48*, 1644–1653.

Lee, C.Y., Sher, H.F., Chen, H.W., Liu, C.C., Chen, C.H., Lin, C.S., Yang, P.C., Tsay, H.S., and Chen, J.J. (2008). Anticancer effects of tanshinone I in human non-small cell lung cancer. Mol. Cancer Ther. *7*, 3527–3538.

Lee, N.Y., Choi, H.K., Shim, J.H., Kang, K.W., Dong, Z., and Choi, H.S. (2009). The prolyl isomerase Pin1 interacts with a ribosomal protein S6 kinase to enhance insulin-induced AP-1 activity and cellular transformation. Carcinogenesis *30*, 671–681.

Misaghi, S., Balsara, Z.R., Catic, A., Spooner, E., Ploegh, H.L., and Starnbach, M.N. (2006). Chlamydia trachomatis-derived deubiquitinating enzymes in mammalian cells during infection. Mol. Microbiol. *61*, 142–150.

Monje, P., Hernández-Losa, J., Lyons, R.J., Castellone, M.D., and Gutkind, J.S. (2005). Regulation of the transcriptional activity of c-Fos by ERK. A novel role for the prolyl isomerase PIN1. J. Biol. Chem. *280*, 35081–35084.

Moulder, J.W. (1991). Interaction of chlamydiae and host cells in vitro. Microbiol. Rev. *55*, 143–190.

Mukherjee, S., Keitany, G., Li, Y., Wang, Y., Ball, H.L., Goldsmith, E.J., and Orth, K. (2006). Yersinia YopJ acetylates and inhibits kinase activation by blocking phosphorylation. Science *312*, 1211–1214.

O'Connor, T.J., Adepoju, Y., Boyd, D., and Isberg, R.R. (2011). Minimization of the Legionella pneumophila genome reveals chromosomal regions involved in host range expansion. Proc. Natl. Acad. Sci. USA *108*, 14733–14740.

Park, J.E., Lee, J.A., Park, S.G., Lee, D.H., Kim, S.J., Kim, H.J., Uchida, C., Uchida, T., Park, B.C., and Cho, S. (2012). A critical step for JNK activation: isomerization by the prolyl isomerase Pin1. Cell Death Differ. *19*, 153–161.

Peters, J., Wilson, D.P., Myers, G., Timms, P., and Bavoil, P.M. (2007). Type III secretion à la Chlamydia. Trends Microbiol. *15*, 241–251.

Rajalingam, K., Sharma, M., Lohmann, C., Oswald, M., Thieck, O., Froelich, C.J., and Rudel, T. (2008). Mcl-1 is a key regulator of apoptosis resistance in Chlamydia trachomatis-infected cells. PLoS ONE *3*, e3102.

Rejman Lipinski, A., Heymann, J., Meissner, C., Karlas, A., Brinkmann, V., Meyer, T.F., and Heuer, D. (2009). Rab6 and Rab11 regulate Chlamydia trachomatis development and golgin-84-dependent Golgi fragmentation. PLoS Pathog. *5*, e1000615.

Rohmer, L., Hocquet, D., and Miller, S.I. (2011). Are pathogenic bacteria just looking for food? Metabolism and microbial pathogenesis. Trends Microbiol. *19*, 341–348.

Schonthaler, H.B., Guinea-Viniegra, J., and Wagner, E.F. (2011). Targeting inflammation by modulating the Jun/AP-1 pathway. Ann. Rheum. Dis. *70* (*Suppl 1*), i109–i112.

Wang, W., Shi, L., Xie, Y., Ma, C., Li, W., Su, X., Huang, S., Chen, R., Zhu, Z., Mao, Z., et al. (2004). SP600125, a new JNK inhibitor, protects dopaminergic neurons in the MPTP model of Parkinson's disease. Neurosci. Res. *48*, 195–202.

Wang, A., Al-Kuhlani, M., Johnston, S.C., Ojcius, D.M., Chou, J., and Dean, D. (2012). Transcription factor complex AP-1 mediates inflammation initiated by Chlamydia pneumoniae infection. Cell. Microbiol. *15*, 779–794.

Xia, M., Bumgarner, R.E., Lampe, M.F., and Stamm, W.E. (2003). Chlamydia trachomatis infection alters host cell transcription in diverse cellular pathways. J. Infect. Dis. *187*, 424–434.

Yen, H.C., Xu, Q., Chou, D.M., Zhao, Z., and Elledge, S.J. (2008). Global protein stability profiling in mammalian cells. Science *322*, 918–923.

Zhong, G. (2011). Chlamydia trachomatis secretion of proteases for manipulating host signaling pathways. Front Microbiol *2*, 14.